JOURNAL OF COMPUTATIONAL PHYSICS 34, 74-93 (1980)

Numerical Solutions of Chemically Reacting Flows in Porous Media*

R. C. Y. CHIN AND R. L. BRAUN

University of California, Lawrence Livermore Laboratory, Livermore, California 94550

Received July 20, 1978

We discuss the computational aspects of a porous flow past a reacting solid undergoing pyrolysis. We present governing equations and develop an accurate numerical method for their solution. The algorithm accurately calculates the rapidly varying component and uses a fixed step size commensurate with the smoothly varying component of the solution. The resulting nonlinear equation is solved with Newton's method; the linear system is solved using a discrete analog of the invariant-imbedding method for second-order, linear, two-point boundary-value problems. We also develop a criterion for truncating the computational domain to minimize the calculational effort, and we present some typical calculations showing that the scheme is accurate and efficient.

INTRODUCTION

Energy resource recovery processes such as oil shale retorting and coal gasification belong to the class of chemically reacting, porous-medium flow phenomena. Inherent in these phenomana are problems that arise from the disparate time scales of the physical and chemical processes. We have developed a one-dimensional mathematical model [1] that simulates the chemico-physical processes involved in concurrent vertical retorting of rubblized oil shale.

The processes are modeled by a set of stiff differential equations. (Such a system is considered stiff on some interval if a component of the solution exists that rapidly varies within the interval. [2])

Work continues on this model, which is intended to be a comprehensive retorting model that includes all of the important chemico-physical processes.

To illustrate the basic difficulties and the current techniques for solution, we consider the numerical solution of a simplified retorting problem. In the simplified problem, part of the solid material (S) undergoes thermal decomposition at elevated temperatures or pryolysis to form a gaseous effluent (G_1) and a solid residue (S_1). The physical processes involved are axial convective transport of energy and mass from the bulk gas flow, the effective axial conductive transport of heat, and heat transfer between the gas stream and the solid.

Solving the governing equations with our numerical method results in a nonlinear system of equations. The nonlinear equation is solved with Newton's method and the

* This work was performed under the auspices of the U.S. Department of Energy by Lawrence Livermore Laboratory under contract No. W-7405-Eng-48.

0021-9991/80/010074-20$02.00/0

linear system with a discrete analog of the invariant-imbedding method for second-order, linear, two-point boundary-value problems. This approach was inspired by a lecture of G. H. Meyer on using invariant-imbedding algorithms in free-boundary problems.

Governing Equations

The governing equations for the simple retorting problem are:

The energy equation for the solid:

$$\rho_S C_S \frac{\partial T}{\partial t} = \frac{3h}{r_0}(T_g - T) - h_1 kS. \tag{1}$$

The solid species continuity equation:

$$\frac{\partial S}{\partial t} = -kS. \tag{2}$$

The energy equation for the gas:

$$\frac{\partial}{\partial z} k_e \frac{\partial T_g}{\partial z} = CG \frac{\partial T_g}{\partial z} + \frac{3h\alpha}{r_0}(T_g - T). \tag{3}$$

The gas species continuity equation:

$$\frac{\partial G_1}{\partial z} = f_1 kS. \tag{4}$$

Here, T is the solid temperature, S is the reacting species, T_g is the gas temperature, and G_1 is the gaseous reaction product.

Augmenting the governing equation, we have the following subsidiary relations:

$$\begin{aligned} G &= G_0 + G_1, \\ C &= C(T_g), \\ h &= h(T_g), \\ \rho &= \rho_0 + S, \\ C_S &= C_S(T), \\ k &= k(T) = Ae^{-E/T}, \end{aligned}$$

where A and E are constants. Here, G is the superficial gas-flow rate, C is the specific heat of the gas, h is the heat-transfer coefficient, ρ is the density of the solid, C_S is the specific heat of the solid, ρ_0 is the density of the nonreacting solid, and G_0 is the input superficial gas-flow rate.

Initial conditions for the problem are

$$S(z, 0) = S_0(z) \qquad \text{and} \qquad T(z, 0) = T_0(z), \qquad 0 < z < L;$$

boundary conditions are

$$T_g(0, t) - \frac{k_e}{CG} \frac{\partial T_g}{\partial z} (0, t) = g(t),$$

$$\frac{\partial T_g}{\partial z} (L, t) = 0,$$

$$G_1(0, t) = 0, \qquad t > 0.$$

We see from these equations that the gas-solid heat-transfer process constitutes one of the characteristic time scales of interest. At low temperatures, this is the dominant phenomenon. As temperature increases, pyrolysis occurs and the pyrolysis-reaction rate becomes comparable to the heat-transfer rate, surpassing it at higher temperatures. With large reaction rates, only a small amount of reactant remains. Because of the form of the reaction-rate expression, the decomposition occurs over a very narrow temperature range. The temperature variations (both solid and gaseous) are smoother than that of the solid species profile. Disparate scales of variation occur in the solution, creating a stiff system of partial differential equations in the sense Miranker [2] described.

An obvious implication of the theory of numerical solutions for stiff, ordinary differential equations is that a stiffly stable algorithm with dynamic step-size control is required to integrate the equations if strict accuracy is to be maintained. Dynamic step-size control in space and time can be most difficult to implement.

In this paper, we develop a scheme that uses a fixed step size commensurate with the smooth temperature variation and yet calculates accurately the rapidly varying species profile. In the next section, we develop a nonlinear discretization of Eq. (2) (in contrast to a linear multistep method) that relates accurately the rapidly varying species concentration to the smoother solid temperature change. In so doing, the stiff aspect of the problem is eliminated in that the reduced problem is concerned with calculating the smoothly varying gaseous and solid temperature profiles.

In developing the nonlinear discretized analog of the species continuity equation, we take advantage of the form of the equation and of the interpolation property of the smoothly varying temperature profile. An error estimate is also derived.

Discretization of Species Continuity Equation

To begin, consider the integration of the first-order rate equation

$$\frac{\partial S}{\partial t} = -k(T)\, S \tag{5}$$

for

$$t \in I_n = (t_{n-1}, t_n), \qquad \text{given } S(t_{n-1}) = S^{n-1}.$$

Formally, we have

$$\ln \frac{S(t)}{S^{n-1}} = -\int_{t_{n-1}}^{t} [k(T)](t')\, dt', \qquad t < t_n, \tag{5'}$$

with $k(T) = Ae^{-E/T}$. If $T(t)$ is invertible, i.e., $t = f(T)$, then

$$\ln \frac{S(t)}{S^{n-1}} = -\int_{T^{n-1}}^{T} k(T) \frac{dt}{dT}\, dT \qquad \text{for} \quad T^{n-1} < T < T^n.$$

Suppose, $T(t)$ has a linear interpolation for $t \in I_n$, i.e.,

$$T(t) = T^{n-1} + \frac{T^n - T^{n-1}}{t_n - t_{n-1}} (t - t_{n-1}) + O[(t_n - t_{n-1})^2], \tag{6}$$

then the integral on the right may be evaluated via the exponential integral

$$E_1(z) = \int_z^\infty x^{-1} e^{-x}\, dx$$

to yield

$$\int_{T^{n-1}}^{T^n} k(T) \frac{dt}{dT}\, dT$$

$$\cong \frac{\tau}{\Delta T} \{T^n k(T^n) - T^{n-1} k(T^{n-1}) + AE[E_1(E/T^n) - E_1(E/T^{n-1})]\}, \tag{7}$$

where

$$\tau = t_n - t_{n-1} \qquad \text{and} \qquad \Delta T = T^n - T^{n-1}.$$

The solution of Eq. (5) is then

$$S_n = S_{n-1} \exp\{-(t_n - t_{n-1})\, I_0(T^n, T^{n-1})/\Delta T\}, \tag{8}$$

where, for convenience, we have set

$$I_0(T^n, T^{n-1}) = T^n k(T^n) - T^{n-1} k(T^{n-1}) - AE[E_1(E/T^n) - E_1(E/T^{n-1})].$$

From the derivation, we see that the accuracy of the integration of Eq. (1) depends entirely upon the extent to which $T(t)$ may be approximated by a linear function for $t \in I_n$. The error estimate is summarized as follows:

THEOREM. *Suppose $T(t)$ has a linear interpolation for $t_0 < t < t_1$ such that*

$$T(t) = T_0 + \frac{\Delta T}{\tau} (t - t_0) + \frac{T_C''}{2} (t - t_0)(t - t_1),$$

where

$$T_i = T(t_i), \qquad i = 0, 1,$$

$$T_C'' = T''(t_C), \qquad t_0 < t_C < t_1,$$

then for

$$2\,\frac{\tau^2 T_c''}{\Delta T}\left(\frac{E}{\Delta T}\right)\left[1 + \frac{T_1 + T_0}{2E}\right] \ll 1,$$

$$\int_{t_0}^{t_1} k\; T(t)\,dt = \frac{\tau}{\Delta T}\, I_0(T_1, T_0)\,\Bigg\{1 + \frac{\tau^2 T_c''}{\Delta T}\left(\frac{E}{\Delta T}\right)$$

$$\times\left[1 + \left(\frac{T_1 + T_0}{2E}\right)[T_1 k(T_1) - T_0 k(T_0)] - \frac{1}{2}\left(1 + \frac{T_1 + T_0}{E}\right)\right.$$

$$\left.\times\, AE[E_1(E/T_1) - E_1(E/T_0)]\right]\Big/ I_0(T_1, T_0) + O(\tau^4)\Bigg\},$$

where

$$E_1(z) = \int_z^\infty e^{-\tau}\,dt/t.$$

The proof of the theorem mimics the error analysis for steepest descent methods. (See Olver [3].) Higher-order methods can be generated with a higher-order interpolation for $T(t)$, but the price paid is the computation of the incomplete gamma functions that result.

An integration procedure of this type, Eq. (5), has been proposed by Dennis [4] for integrating ordinary differential equations possessing exponential-type solutions. We must also include the exponential fitting methods [2, 5, 6] in this category. The integral

$$\int_{t_{n-1}}^{t_n} k(T)\,dt$$

is numerically troublesome because of the form of $k(T)$. This recognition is new and contributes to the state of the art. For computational purposes, we use a rational approximation for the exponential integral $E_1(x)$, [7], i.e.,

$$xe^x E_1(x) = \frac{x^2 + a_1 x + a_2}{x^2 + b_1 x + b_2} + \epsilon(x),$$

where

$$a_1 = 2.334733, \qquad b_1 = 3.330657,$$

$$a_2 = 0.250621, \qquad b_2 = 1.681534,$$

and

$$|\,\epsilon(x)| < 5 \times 10^{-5} \qquad \text{for} \quad 1 \leqslant x \leqslant X.$$

The term $I_0(T^n, T^{n-1})$ may be rewritten as

$$\frac{1}{T^n - T^{n-1}} \{T^n k(T^n)\, \tilde{E}_1(E/T^n) - T^{n-1} k(T^{n-1})\, \tilde{E}_1(E/T^{n-1})\}, \tag{9}$$

where

$$\tilde{E}_1(x)\, \frac{0.995924x + 1.430913}{x^2 + 3.33065x + 1.681534}.$$

This formula will be used for later discussion.

Formulation of the Difference Scheme and the Computational Algorithm

Difference Scheme

Our basic difference scheme is the trapezoidal rule, which is formally second-order accurate. Keller [8] has adopted variants of the trapezoidal rule to study parabolic equations with great success. The derivation of the difference equation in this section closely follows Keller's method.

Consider a partitioning of the domain $D = \{z, t \mid 0 < z < L, 0 < t\}$ such that

$$\begin{aligned} \Delta_j &= z_j - z_{j-1}, & 1 < j < N; \\ \tau_n &= t_n - t_{n-1}, & 1 < n; \end{aligned}$$

with

$$t_0 = 0 \qquad z_0 = 0, \qquad \text{and} \qquad z_N = L.$$

Let

$$\begin{aligned} \phi^n(z) &= \phi(z, t_n), \\ (D_t^- \phi^n)(z) &= \tau_n^{-1}(\phi^n - \phi^{n-1}), \\ \phi^{n-1/2}(z) &= 1/2(\phi^n + \phi^{n-1}). \end{aligned}$$

Applying the trapezoidal rule to Eq. (1), we obtain

$$(\rho_S C_S)^{n-1/2}\, D_t^- T^n - h_1 D_t^- S^n = \frac{3}{2r_0} [h(T_g - T)]^{n-1/2}. \tag{10}$$

By definition,

$$f^{n-1}(z) = \frac{1}{2} (C_S \rho_S T)^{n-1} - h_1 S^{n-1} - \frac{3\tau_n}{2} h^{n-1}(T_g^{n-1} - T^{n-1}).$$

Equation (10) becomes

$$F_1^n(z) = (\rho_S C_S)^{n-1/2}\, T^n - \frac{1}{2} (C_S \rho_S)^n\, T^{n-1} - h_1 S^n - \frac{3\tau_n}{2r_0} h^n (T_g - T)^n - f^{n-1} = 0,$$

$$n = 1, 2, \ldots \qquad \text{and} \qquad 0 < z < L. \tag{11}$$

Adjoining Eq. (10), we have

$$\begin{aligned} S^n(z) &= S^{n-1}(z) \exp[-\tau_n I_0(T^n, T^{n-1})/\Delta T], \qquad n = 1, 2, \ldots; \\ \rho_S{}^n &= \rho_S(S^n); \\ C_S{}^n &= C_S(T^n); \\ h^n &= h(T_g{}^n). \end{aligned} \tag{12}$$

In principle, Eqs. (11) and (12) may be solved for $T^n(z)$ in terms of $T_g{}^n(z)$, i.e.,

$$T^n(z) = T^n(T_g{}^n; T^{n-1}, T_g^{n-1}, S^{n-1}). \tag{13}$$

After substituting the relation of Eq. (13) into Eq. (3), we have reduced the original problem to solving a nonlinear, two-point boundary problem for $T_g{}^n(z)$. This observation is germane to the development of the computational algorithm to be discussed.

We will now turn to the discretization of Eq. (3). As in Keller, we employ the notation

$$\begin{aligned} \phi_j{}^n &= \phi(z_j, t_n), \\ \phi_{j\pm1/2}^n &= 1/2(\phi_j{}^n + \phi_{j\pm1}^n), \\ D_z{}^-\phi_j{}^n &= \Delta_j^{-1}(\phi_j{}^n - \phi_{j-1}^n). \end{aligned}$$

The trapezoidal rule will be applied to the integration of Eq. (3), which is written as a system of first-order, partial-differential equations, i.e.,

$$\begin{aligned} (k_e) \frac{\partial T_g{}^n}{\partial z} &= P^n, \\ \frac{\partial P^n}{\partial z} &= (CG)^n \frac{\partial T_g{}^n}{\partial z} + \frac{3h}{r_0}(T_g{}^n - T^n), \end{aligned} \tag{14}$$

to yield

$$\begin{aligned} F_{2,j}^n &= (k_e)_{j-1/2}\, D_z{}^-(T_g)_j^n - P_{j-1/2}^n = 0, \qquad j = 1, 2, \ldots, N \\ F_{3,j}^n &= D_z{}^-P_j{}^n - (CG)_{j-1/2}^n\, D_z{}^-(T_g)_j^n - \frac{3\alpha}{r_0}[h(T_g - T)]_{j-1/2}^n = 0, \qquad j = 1, 2, \ldots, N. \end{aligned} \tag{15}$$

Similarly, we obtain the following discrete analog of Eq. (4):

$$G_{1_j}^n = G_{1_{j-1}}^n + \frac{\Delta z}{2} f_1[(kS)_j^n + (kS)_{j-1}^n];$$

$G_{n_j}^1$ appears in Eq. (15) through

$$G_j{}^n = G_0 + G_{1_j}^n.$$

The initial and boundary conditions are

$$\begin{aligned} &T_j^0 = T_0(z_j), \qquad j = 0, 1, 2, \ldots, N, \\ &T^n_{g,0} - \frac{1}{(CG)^n_0} P_0{}^n = g(t^n), \qquad (16) \\ &G^n_{1_0} = 0, \end{aligned}$$

and

$$P_N{}^n = 0, \qquad n = 1, 2, \ldots .$$

The initial values $\{T^0_{g,j}\}$ are obtained by solving Eq. (14). The boundary values $\{T_0{}^n\}$ are computed simultaneously by combining Eq. (11) evaluated at $z = 0$ to the interior set of difference equations. Thus, at a given time level t_n, we have a system of $4N + 3$ equations [Eqs. (11), (12), and (15)] for the variables, $S_j{}^n$, $T_j{}^n$, $T_g{}^n$, $j = 0, 1, 2, \ldots, N$ and $P_j{}^n$, $j = 0, 1, \ldots, N - 1$. This system is reducible by substituting Eq. (12) into Eq. (11) to give $3N + 2$ equations. The problem now is to determine the roots of the equations

$$\mathbf{G}(\mathbf{x}) = \begin{bmatrix} F^n_{1,0} \\ \vdots \\ F^n_{1,N} \\ -g(t^n) + T_0{}^n + \dfrac{1}{(CG)^n_0} P_0{}^n \\ \vdots \\ F^n{}_{,N} \\ F^n_{3,1} \\ \vdots \\ F^n_{3,N} \end{bmatrix} = \mathbf{0}, \tag{17}$$

where

$$\mathbf{x}^T = [\{T_j{}^n\}, 0 \leqslant j \leqslant N, \{T^n_{g,j}\}, 0 \leqslant j \leqslant N, \{P_j{}^n\}, 0 \leqslant j \leqslant N - 1].$$

Using an earlier observation on Eq. (13), the system can be further reduced to $2N + 1$ nonlinear equations in the variables $\{T^n_{g,j}\}$ and $\{P_j{}^n\}$. We use Newton's scheme to solve these equations.

Newton's Scheme and the Computational Algorithm

Applying Newton's method to the solution, Eq. (17) gives

$$\mathrm{J}^{(m)} \Delta x = -G^{(m)}, \tag{18}$$

where

$$\mathrm{J}^{(m)} = \frac{\partial \mathbf{G}}{\partial \mathbf{x}} (\mathbf{x}^m) \qquad \text{the Jacobian matrix,}$$

$$\Delta \mathbf{x} = \mathbf{x}^{(m+1)} - \mathbf{x}^{(m)},$$

$$m = \text{iteration index.}$$

Moreover, the Jacobian matrix J has the structure

$\underline{\underline{J}} =$

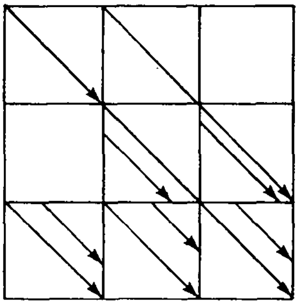

⊙

Clearly, the system of linear equations in Eq. (18) is reducible. By joining the boundary condition $P_N{}^n = 0$ to the reduced set and reordering the variables and the equations, the reduced problem

$$J'^{(m)} \Delta x' = -G'^{(m)} \tag{19}$$

is of dimension $2(N+1)$. The matrix J′ is block tridiagonal with 2×2 blocks. Let

$$u_j = T^n_{g,j}$$

and

$$p_j = p_j{}^n.$$

Then

$$\Delta \mathbf{x}' = \begin{bmatrix} \Delta u_0 \\ \Delta p_0 \\ \Delta u_1 \\ \vdots \\ \Delta u_j \\ \Delta p_j \\ \vdots \\ \Delta u_n \\ \Delta p_N \end{bmatrix}, \qquad \mathbf{G} = \begin{bmatrix} F^n_{2,0} \\ F^n_{2,1} \\ D_{1/2} \\ \\ D_{j-1/2} \\ F^n_{2,j-1} \\ \vdots \\ D_{N-1/2} \\ 0 \end{bmatrix},$$

and

$$J' = \begin{bmatrix} A_0 & C_0 & & \\ B_1 & A_1 & C_1 & \\ & \ddots & \ddots & \ddots \\ & & & C_{N-1} \\ & & B_N & A_N \end{bmatrix},$$

where we have introduced

$$\mathsf{A}_0 = \begin{bmatrix} 1 & -\dfrac{1}{(CG)_0} \\ \kappa_{1/2} & 1 \end{bmatrix},$$

$$\mathsf{A}_j = \begin{bmatrix} a_{j-1/2} & -1 \\ \kappa_{j+1/2} & 1 \end{bmatrix}, \qquad j = 1, 2, \dots, N-1,$$

$$\mathsf{A}_N \quad \begin{bmatrix} a_{N-1/2} & -1 \\ 0 & 1 \end{bmatrix},$$

$$\mathsf{C}_j = \begin{bmatrix} 0 & 0 \\ -\kappa_{j+1/2} & 1 \end{bmatrix}, \qquad j = 0, 1, 2, \dots, N-1,$$

$$\mathsf{B}_j = \begin{bmatrix} -b_{j-1/2} & 1 \\ 0 & 0 \end{bmatrix}, \qquad j = 1, 2, \dots, N.$$

Clear discussions of the numerical solution of the linear system in Eq. (19) are found in Keller [8] and Varah [9, 10]. Keller applied the standard block LU-decomposition algorithm [11]. Varah extended the block-factorization technique further and compared its efficiency with the efficiency of band-solving methods when the matrix is treated as a band matrix. Other methods of solution also exist.

Construction of a factorization method analogous to the method of invariant imbedding [12, 13] for solving linear two-point boundary-value problems is possible [14] because:

— Equations (13), (14), and (16) comprise a nonlinear, two-point boundary-value problem that can be solved by quasi-linearization techniques using invariant imbedding to find the solution to the linearized problem.

— The proposed method of solution using Newton's scheme is just the discrete analog of the factorization method, and it is reasonable to expect the discrete form of invariant imbedding to lead to a solution algorithm for Eq. (19).

Moreover, the factorization method induced by invariant imbedding gives a direct identification of the physical variables. This together with the fact that invariant imbedding method is an initial-value technique make it most suitable for free-boundary problems [15, 16] and for developing a dynamic domain truncation algorithm to follow in a later section.

The essential ingredient of the invariant-imbedding method is the Riccati transformation. Its discrete analog applicable to Eq. (19) is

$$\Delta u_i = R_i \, \Delta p_i + S_i, \qquad i = 0, 1, 2, \dots, N. \tag{20}$$

Substituting Eq (20) into (19), we obtain a factorization algorithm, whose forward sweep is

$$R_0 = \frac{1}{(CG)_0^n}, \qquad S_0 = -F_{2,0}^n,$$

$$\begin{aligned} W_i &= \kappa_{i-1/2} + a_{i-1/2} + [\kappa_{i-1/2}(a_{i-1/2} - b_{i-1/2})]\, R_{i-1}, \\ R_i &= 2 + \{[\kappa_{i-1/2} - b_{i-1/2}]\, R_{i-1}\}/W_i, \\ S_i &= \{[b_{i-1/2} + \kappa_{i-1/2}]\, S_{i-1} - [b_{i-1/2}R_{i-1} - 1]\, F_{2,i}^n \\ &\qquad + [\kappa_{i-1/2}R_{i-1} + 1]\, D_{i-1/2}\}/W_i, \end{aligned} \tag{21}$$

and whose backward sweep is

$$\Delta p_N = 0,$$

$$[\kappa_{i-1/2}R_{i-1} + 1]\, \Delta p_{i-1} = [\kappa_{i-1/2}R_i - 1]\, \Delta p_i + \kappa_{i-1/2}(S_i - S_{i-1}) - F_{2,i}^n,$$
$$i = N, N-1, \ldots, 1.$$

Equation (20) is then used to compute Δu_i, $i = 0, 1, 2, \ldots, N$.

When the block LU-decomposition algorithm [8] is applied to the solution of Eq. (19), the forward sweep is

$$\xi_0 = 1, \qquad \eta_0 = \frac{1}{(CG)_0^n}, \qquad \Delta_0 = \xi_0 - \kappa_{1/2}\eta_0,$$

$$g_0 = -\frac{1}{\Delta_0}(F_{2,0}^n - \eta_0 F_{2,1}^n),$$

$$h_0 = \frac{1}{\Delta_0}[\kappa_{1/2}F_{2,0}^n - \xi_0 F_{2,1}^n],$$

$$\begin{aligned} \xi_i &= a_{i-1/2} + \kappa_{i-1/2}[\xi_{i-1} + b_{i-1/2}\eta_{i-1}]/\Delta_{i-1}, \\ \eta_i &= -\{1 + [\xi_{i-1} + b_{i-1/2}\eta_{i-1}]/\Delta_{i-1}\}, \qquad i = 1, 2, \ldots, N, \\ \Delta_i &= \xi_i - \kappa_{i-1/2}\eta_i, \end{aligned}$$

$$g_i = \frac{1}{\Delta_i}[D_{i-1/2} + b_{i-1/2}g_{i-1} - h_{i-1} - \eta_i F_{2,i+1}^n],$$

$$h_i = -\frac{1}{\Delta_i}\{\kappa_{i+1/2}[D_{i-1/2} + b_{i-1/2}g_{i-1} - h_{i-1}] + \xi_i F_{2,i+1}^n\}, \qquad i = 1, 2, \ldots, N-1,$$

$$g_n = \frac{1}{\Delta_N}[D_{N-1/2} + b_{N-1/2}g_{N-1} - h_{N-1}],$$

$$h_N = 0,$$

and the backward sweep is

$$\begin{aligned} \Delta u_N &= \Delta g_N, \qquad \Delta p_N = h_N = 0, \\ \Delta u_i &= g_i - \eta_i[\kappa_{i-1/2}\, \Delta u_{i+1} - \Delta p_{i+1}]/\Delta_i, \\ \Delta p_i &= h_i + \xi_i[\kappa_{i+1/2}\, \Delta u_{i-1} - \Delta p_{i+1}]/\Delta_i, \qquad i = N-1, N-2, \ldots, 1. \end{aligned}$$

Note that h_i, $i = 0, 1, 2, \ldots, N$ may be computed alternatively as

$$h_i = -[\kappa_{i+1/2}\, g_i + F_{2,i+1}^n].$$

The relation between these two algorithms can be easily found. They are given by

$$\begin{aligned} R_i &= -\eta_i/\xi_i, \\ S_i &= \xi_i^{-1}[g_i \Delta_i - \eta_i F_{2,i+1}^n], \qquad i = 0, 1, 2, \ldots, N. \end{aligned} \tag{22}$$

The discrete invariant-imbedding algorithm is more compact; it has a lesser storage requirement but, essentially, maintains the same operation counts. In general, by virtue of Eq. (22) and the results of Babuška [14], the invariant-imbedding algorithm is expected to be stable whenever the LU-decomposition algorithm is stable.

Initial Estimates

To initiate Newton's scheme at $t = t_n$, we use the previous values at $t = t_{n-1}$. A first-order forward Euler formula predicts the initial estimate for S_i^n, called $(S_i^n)^0$. Because $S_i^n \geqslant 0$ for all i and n, $(S_i^n)^0$ is set to zero if the computed value is negative. They are then substituted into Eq. (11) along with T_g evaluated at $t = t_{n-1}$ to yield the initial estimates of T_i^n, called $(T_i^n)^0$. In turn, Eq. (15) is solved using $(T_i^n)^0$ and $(S_i^n)^0$. To avoid solving a nonlinear, two-point boundary-value problem, we evaluate the gaseous specific heat C and the heat-transfer coefficient h at $t = t_{n-1}$ and solve the resultant linear problem for $(T_{g,i}^n)^0$. The discrete invariant-imbedding algorithm is applied toward its solution.

Truncation of Computational Domain

Physically, the retorting front propagates with a finite speed and spreads in time, exhibiting a wavelike structure. An efficient computational algorithm takes advantage of this in truncating the computational domain. Determining the criterion for truncating the domain requires insights into the structure of the solution, particularly the solution ahead of the decomposition or retorting front.

Because the rate expression in the decomposition reaction is of the Arrhenius type and the solution has wavelike behavior, we expect that, at a given time t, there is a point $z = \bar{z}(t)$ such that $S(z, t) \sim S(z, 0)$ for $z > \bar{z}$. This is to say that the solid species S has not yet decomposed appreciably. From the gas-species conservation equation, it follows that the flow is fixed at $G(\bar{z}, t)$. Moreover, if the specific heat C, the heat-transfer coefficient h, and the heat conductivity k_e are weak functions of their respective temperature, the following approximate equations result:

$$\begin{aligned} \rho_S C_S \frac{\partial T_S}{\partial t} &= \frac{3h}{r_0}(T_g - T_S), \\ \frac{\partial}{\partial z} k_e \frac{\partial T_g}{\partial z} &= CG \frac{\partial T_g}{\partial z} + \frac{3h\alpha}{r_0}(T_g - T_S) \end{aligned} \tag{23}$$

for $z > \bar{z}(t)$ and $t > 0$. The equations are linear. Using the wave-front analysis of Whitham, [17] we find that the wave-front propagates with a speed

$$\nu_S = \frac{CG}{\rho_S C_S \alpha},$$

and, in the neighborhood of the wave-front, the solution is governed by

$$\frac{3h\alpha}{r_0} \frac{\partial T_g}{\partial t} = \left\{\frac{CG}{\nu_S} + \left[\frac{3hk_e}{C_S \rho_S r_0} \frac{1}{\nu_S{}^2}\right]\right\} \frac{\partial^2 T_g}{\partial \xi^2} + \frac{k_e}{\nu_S{}^2} \frac{\partial^3 T_g}{\partial \xi^3}, \tag{24}$$

where $\xi = t - z/\nu_S$. We may solve Eq. (24) to set up a truncation criterion. The solution of Eq. (24) having the desirable property is given by

$$\begin{aligned} T_g(\xi, t) &= \frac{T_0}{2\pi} \int_{-\infty}^{\infty} \exp(-(\alpha_0 k^2 + i\beta_0 k^3)\, t + ik\xi) \frac{dk}{k} \\ &= T_0\{\tfrac{1}{2} - A_{i_{3,2}}[\alpha_0 t^{1/3} \beta_0^{-2/3}, -\xi(\beta_0 t)^{-1/3}]\}, \end{aligned} \tag{25}$$

where

$$\alpha_0 = \left(\frac{CG}{\nu_S} + \frac{3hk_e}{C_S \rho_S r_0} \frac{1}{\nu_S{}^2}\right)\left(\frac{3h\alpha}{r_0}\right)^{-1},$$

$$\beta_0 = k_e \left(\nu_S{}^2 \frac{3h\alpha}{r_0}\right)^{-1},$$

$$A_{i_{3,2}} = \text{the generalized Airy function.}$$

The relation in Eq. (25) is valid away from $z = L$. A possible criterion may be to truncate the computational domain when

$$\frac{T_g}{T_0}(\bar{\xi}, t) = 1 + \epsilon$$

or to find $\bar{\xi}$ such that

$$\tfrac{1}{2} + \epsilon = A_{i_{3,2}}[\alpha_0 t^{1/3} \beta_0^{-2/3}, -\bar{\xi}(\beta_0 t)^{-1/3}].$$

Unfortunately, to apply this criterion we need to compute the generalized Airy function of indices 3, 2 or to have a table of this function [18]. Neither of these techniques is acceptable computationally. The former requires additional computation time, while the latter puts demands on storage. It would be desirable to do the truncation estimation within the computational algorithm.

In view of this discussion, it is clear that the truncation of domain must occur for $S_i^n \sim S_i^0$ in that portion of the domain where no appreciable decomposition takes place. Let this be called $\tilde{D}_{\epsilon_S}$, i.e., $\tilde{D}_{\epsilon_S} = \{x, t \mid S(x, t) = S(x, 0) : \epsilon_S\}$ with $\epsilon_S > 0$. During the calculation of the initial estimates for $S_i^n - (S_i^n)^0$, we can determine $\tilde{D}^0_{\epsilon_S}$, which approximates $\tilde{D}_{\epsilon_S}$, i.e.,

$$\tilde{D}^0_{\epsilon_S} = \{i, n \mid (S_i^n)^0 = S_i^0 + \epsilon_S\}.$$

The next step is to derive a meaningful criterion to determine the cutoff.

During the third stage of the prediction cycle, we use the discrete invariant-imbedding algorithm to solve a two-point boundary-value problem for

$$\{(T_i^n)^0\}_{i=0}^N,$$

i.e.,

$$(T_i^n)^0 = \tilde{R}_i(P_i^n)^0 + \tilde{S}_i,$$

$$\tilde{R}_i = \left(2 + \left\{\kappa_{i-1/2} - \left[CG_{i-1/2} - \frac{3\alpha\,\Delta z}{2r_0}\,h_{i-1/2}\right]\right\}\tilde{R}_{i-1}\right)$$
$$\times\left(CG_{i-1/2} + \frac{3\alpha\,\Delta z}{2r_0}\,h_{i-1/2} + \kappa_{i-1/2} + \kappa_{i-1/2}\frac{3\alpha\,\Delta z}{r_0}\,h_{i-1/2}\tilde{R}_{i-1}\right)^{-1}, \quad (26)$$

$$S_i = \left\{\left[\kappa_{i-1/2} + CG_{i-1/2} - \frac{3\alpha\,\Delta z}{2r_0}\,h_{i-1/2}\right]\tilde{S}_{i-1}\right.$$
$$\left. + \left[\kappa_{i-1/2}R_{i-1} + 1\right]\frac{3\alpha\,\Delta z}{2r_0}\,h_{i-1/2}(T^n_{s_{i-1/2}})^0\right\}$$
$$\times\left[CG_{i-1/2} + \frac{3\alpha\,\Delta z}{2r_0}\,h_{i-1/2} + \kappa_{i-1/2} + \kappa_{i-1/2}\frac{3\alpha\,\Delta z}{r_0}\right]^{-1}. \quad (27)$$

$$[\kappa_{i-1/2}\tilde{R}_{i-1} + 1](P^n_{i-1})^0 = [\kappa_{i-1/2}\tilde{R}_i - 1](P_i^n)^0 + \kappa_{i-1/2}(\tilde{S}_i - \tilde{S}_{i-1}),$$
$$i = N, N-1, \ldots, 1, \quad (28)$$

with

$$\tilde{S}_0 = g(t^n), \qquad \tilde{R}_0 = \frac{1}{(CG)_0^n}, \qquad \text{and} \qquad (P_N^n)^0 = 0.$$

Here,

$$\kappa_{i-1/2} = \frac{2(k_e)_{i-1/2}}{\Delta z}.$$

The solutions of Eqs. (27) and (28), with their associated initial conditions, are given by

$$\tilde{S}_i = g(t^n)\prod_{j=0}^{i-1} a_j + e_{i-1} + \sum_{j=2}^{i} e_{i-j}\left[\prod_{l=0}^{j-2} a_{i-l-1}\right], \qquad 0 \leqslant i \leqslant N, \tag{29}$$

and

$$P_i = d_{i+1} + d_{i+2}C_{i+1} + \sum_{K=3}^{N-i} d_{i+k}\left[\prod_{l=0}^{k-2} C_{i-l+1}\right], \qquad 0 \leqslant i < N, \tag{30}$$

where

$$a_i = \left(\kappa_{i+1/2} + CG_{i+1/2} - \frac{3\alpha\,\Delta z}{2r_0}\,h_{i-1/2}\right)\gamma_i^{-1},$$

$$e_i = \frac{3\alpha\,\Delta z}{2r_0}\,h_{i-1/2}[T^n_{s_{i+1/2}}]^0\,\gamma_i^{-1},$$

$$\gamma_i = \kappa_{i+1/2} + CG_{i+1/2} + \frac{3\alpha\,\Delta z}{2r_0}\,h_{i+1/2}[1 + 2\kappa_{i+1/2}R_i],$$

$$C_i = \frac{\kappa_{i-1/2}R_i - 1}{\kappa_{i-1/2}R_{i-1} + 1},$$

$$d_i = \frac{\kappa_{i-1/2}}{\kappa_{i-1/2}R_{i-1} + 1}\,[\tilde{S}_i - \tilde{S}_{i-1}].$$

Equation (30) suggests the following dynamic truncation algorithm:

(1) Solve Eqs. (26) and (27) for $i = 1, 2, \ldots, N_C$, where N_C is determined by

$$|\,\tilde{S}_{N_C} - \tilde{S}_{N_C-1}\,| \leqslant \epsilon_C \qquad \text{and} \qquad N_C \epsilon \tilde{D}_{\epsilon_s}.$$

(2) Continue solving Eqs. (26) and (27) to $i = N_C + \tilde{N}_C$.

(3) Find the initial condition for the backward recursion of Eq. (28) with

$$(P^n_{N_C})^0 = d_{N_C+1} + d_{N_C+2}C_{N_C+1} + \sum_{k=3}^{\tilde{N}_C} d_{N_C+k}\left[\prod_{l=0}^{k-2} C_{N_C+1+l}\right]. \tag{31}$$

(4) Terminate the subsequent iterative solution at $i = N_C$ with $\Delta P^n_{N_C} = 0$. (Clearly, because of the traveling wavelike behavior of the solution, N_C changes with n.)

An a priori error estimate can be obtained connecting the error ϵ_C with the truncating error associated with Eq. (31). To derive the error estimate, the thermodynamic and transport coefficients must be weak functions of the temperatuie. However, the derivation is lengthy and will not be presented here, although it shows that Eq. (31) gives a reasonable approximation. In general, computational experiences in the next section indicate that the proposed domain-truncation algorithm works.

Numerical Examples

For convenience in computing the example problems, we assume constant gas specific heat, constant heat-transfer coefficient, constant effective axial heat conductivity, and a specific heat for the solid that is a linear function of the solid temperature. The values of the constants are:

$$
\begin{aligned}
G_0 &= 0.01 \text{ kg/m}^2 \text{ sec},\\
h &= 8 \text{ J/m}^2 \text{ Ksec},\\
C &= 1000 \text{ J/kg K},\\
\rho_0 &= 1916 \text{ kg/m}^3,\\
C_S &= 827.4 + 0.922\,(T - 298.) \text{ J/kg K},\\
k(T) &= 2.81 \times 10^{13} \exp\{-26389/\mathrm{T}\} \text{ sec}^{-1},\\
k_e &= 0.25 \text{ J/mKsec},\\
f_1 &= 0.15,\\
h_1 &= 3.7 \times 10^5 \text{ J/kg},\\
r_0 &= 0.01 \text{ m},\\
\alpha &= 0.57,\\
S_0(z) &= 314 \text{ kg/m}^3.
\end{aligned}
$$

A series of problems is solved to assess the effectiveness of the domain truncation algorithm, particularly with the influences of ϵ_S and $\tilde{N}_C$. The results illustrating the effect of ϵ_S with $\tilde{N}_C$ fixed at 10 are summarized in Table I. The effects of varying $\tilde{N}_C$ when ϵ_S is fixed are shown in Table II. From Tables I and II, we see that the value of the temperature gradient P at the domain-truncation point is a function of ϵ_S, provided $\tilde{N}_C$ is large enough that the asymptotic value is reached. For the example problems, $N_C = 10$ gives three-place accuracy to the asymptotic value.

TABLE I

Results of the Domain Truncation Algorithm Showing the Effect of ϵ_S When N_C Is Fixed at 10 and $L = 1.5$, $NZ = 150$, $\Delta t = 300$, and $t = 6000$

ϵ_S	$\tilde{N}_C$	N_C	$P(56)$	$P(64)$	$P(72)$	$P(79)$
10^{-3}	10	56	-7.187×10^{-4}			
10^{-4}	10	64	-7.389×10^{-4}	-7.165×10^{-5}		
10^{-5}	10	72	-7.373×10^{-4}	-7.456×10^{-5}	-6.710×10^{-6}	
10^{-6}	10	79	-7.371×10^{-4}	-7.438×10^{-5}	-7.104×10^{-6}	-8.268×10^{-7}
No domain truncation			-7.370×10^{-4}	-7.435×10^{-5}	-7.073×10^{-6}	-8.672×10^{-7}

TABLE II

Results of the Domain Truncation Algorithm When $\tilde{N}_C$ Is Varied, ϵ_S Is Fixed, and $L = 1.5, NZ = 150, \Delta t = 300$, and $t = 6000$

$\tilde{N}_C$	ϵ_S	N_C	$P(64)$
2	10^{-4}	64	-6.064×10^{-5}
4	10^{-4}	64	-6.996×10^{-5}
6	10^{-4}	64	-7.139×10^{-5}
8	10^{-4}	64	-7.161×10^{-5}
10	10^{-4}	64	-7.165×10^{-5}
No domain truncation			-7.435×10^{-5}

Heuristically, this result is expected from Eq. (31) if $|C_i| < 1$ and $|d_{i+1}| = 0(|d_i|)$, $i \geqslant N_C$. Indeed, for the case in Table II,

$$C_i = -0.6037, \qquad i \geqslant N_C$$

and

$$d_{N_C} > d_{N_C+1} > \cdots > 0.$$

The effects of changing the spatial and time-step sizes on the domain truncation with a fixed $\epsilon_S = 10^{-4}$ and $N_C = 10$ are illustrated in Table III.

TABLE III

Effects of Changes in the Spatial and Time-Step Sizes on the Domain Trunction Algorithm When $\tilde{N}_C = 10$, $\epsilon_S = 10^{-4}$, and $t = 6000$

NZ	Δt	N_C	P	C_{N_C}
150	300	64	-7.538×10^{-5}	-0.6037
150	600	64	-5.951×10^{-5}	-0.6037
300	300	123	-1.671×10^{-4}	-0.3376
300	600	122	-1.515×10^{-4}	-0.3378

To demonstrate the solution behavior of the model equations, a number of calculations are made. Figures 1 through 3 give the gas-temperature profiles, solid-temperature distribution, and the solid-species profile at $t = \frac{1}{4}, \frac{1}{2}$, and 1 day, respectively. To show the difference in scales inherent in the chemico-physical processes, we plot the gas-temperature profile, solid-temperature distribution, and the solid-species profile at $t = 1$ day in Fig. 4. The domain-truncation point is located at $i = 274$ or $z = 1.37$ m. We see from the figures that the solid decomposes within a narrow temperature range 600 to 725 K. Because of the endothermic nature of the decomposition process, the temperature profiles, gas and solid, become smoother in that tempera-

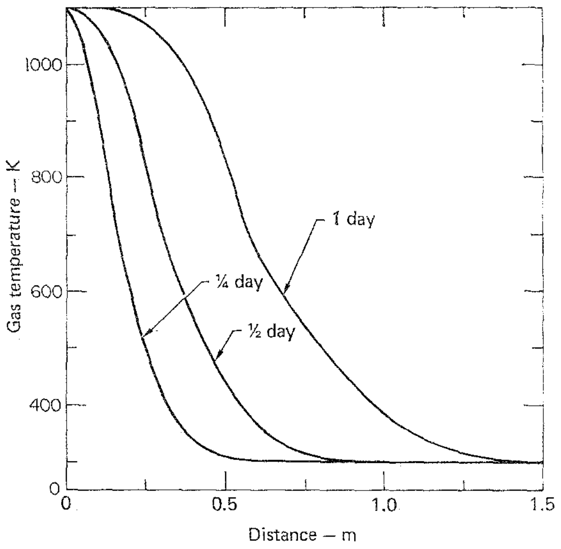

FIG. 1. Gas-temperature profiles $t = \frac{1}{4}, \frac{1}{2}$, and 1 day.

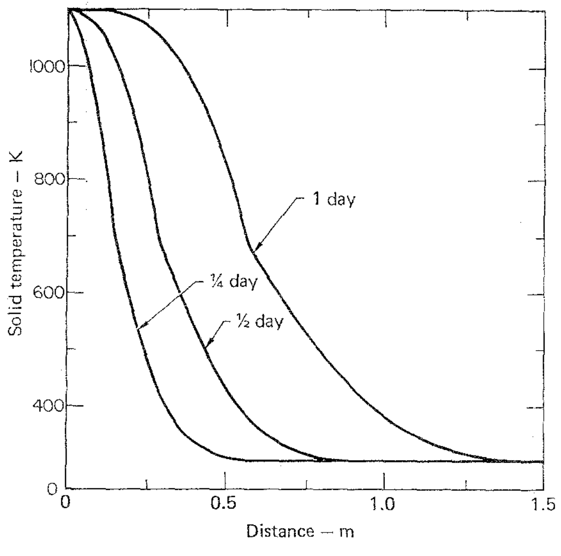

FIG. 2. Solid-temperature distribution $t = \frac{1}{4}, \frac{1}{2}$, and 1 day.

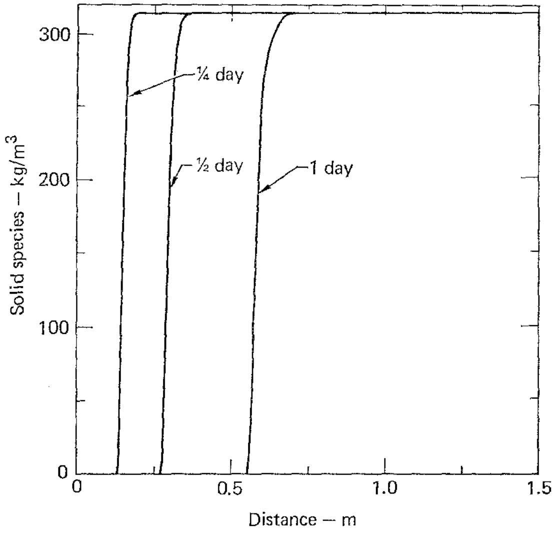

FIG. 3. Solid-species profile at $t = \frac{1}{4}, \frac{1}{2}$, and 1 day.

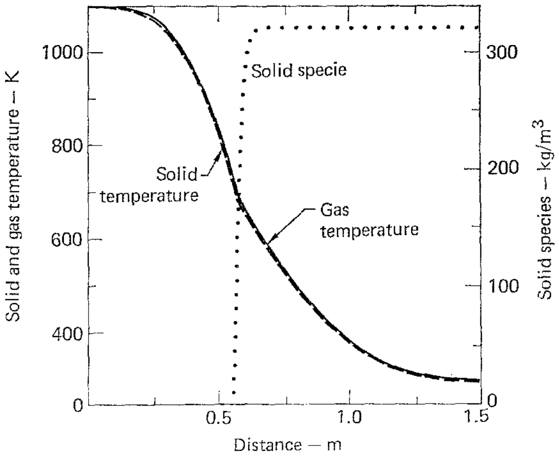

FIG. 4. Gas-temperature profile, solid-temperature distribution, and solid-species profile at $t = 1$ day.

ture range. On the other hand, if the chemical process is exothermic, the temperature variation would steepen from the added chemical energy. In turn, the local species variation will undergo a more drastic change. This case will be a severe test for any numerical scheme, including the present one.

CONCLUSION

We have developed a numerical scheme for modeling specific retorting processes in a rubblized bed of oil shale with a chemically reacting porous medium flow. A nonlinear discretization of the species rate equation is central to the development of the numerical method in recognition of the rapid variation induced by the temperature-dependent decomposition rate. This circumvented the stiffness inherent in the equations with a scheme that uses a fixed step size commensurate with the smooth temperature variation yet also accurately evaluates the rapidly varying species profile.

The numerical method also uses a discrete analog of the invariant-imbedding algorithm for second-order, two-point boundary-value problems to solve the linear system induced by Newton's method. The discrete invariant-imbedding algorithm is further exploited to develop a dynamic domain truncation scheme to increase efficiency.

We have also demonstrated the efficiency of the proposed numerical method by a series of computations that show the scheme is accurate and efficient.

REFERENCES

1. R. L. BRAUN AND R. C. Y. CHIN, Progress report on computer model for in situ oil shale retorting, Lawrence Livermore Laboratory Rept. UCRL-52292, 1977.
2. W. L. MIRANKER, "The Computational Theory of Stiff Differential Equations," Pubblicazioni Serie III -- N. 102 Istituto per le Applicazioni del Calcolo "Mauro Picone," Roma, 1975.
3. F. W. J. OLVER, "Asymptotics and Special Functions," Academic Press, New York, 1974.
4. S. C. R. DENNIS, *Proc. Cambridge Philos. Soc.* **56** (1960), 240–246.
5. P. BROCK AND F. J. MURRAY, *Math. Tables Aids to Comput.* **38** (1952), 63–126.
6. J. CERTAINE, The solution of ordinary differential equations with large time constants, *in* "Mathematical Methods for Digital Computers" (A. Ralston and H. S. Wulf, Eds.), Wiley, New York, 1960.
7. M. ABRAMOWITZ AND I. A. STEGUN, Handbook of mathematic functions. National Bureau of Standards Rept. AMS 55, 1964.
8. H. B. KELLER, "A New Difference Scheme for Parabolic Problems, Numerical Solution of Partial Differencial Equations—II," SYNSPADE 1970 Hubbard, Ed., Academic Press, New York-London, 1971.
9. J. M. VARAH, *Math. Comp.* **26** (1972), 859–868.
10. J. M. VARAH, *Math. Comp.* **28** (1974), 743–755.
11. E. ISAACSON AND H. B. KELLER, "Analysis of Numerical Methods," Wiley, New York, 1966.
12. M. R. SCOTT, "Invariant Imbedding and its Applications to Ordinary Differential Equations, and Introduction," Addison-Wesley, Reading, Mass., 1973.
13. G. H. MEYER, "Initial Value Methods for Boundary Value Problems Theory of Application of Invariant Imbedding," Academic Press, New York/London, 1973.
14. I. BABUŠKA, The connection between the finite difference like methods and the methods based on initial value problems for ODE, in "Numerical Solution of Boundary Value Problems for Ordinary Differential Equations" (A. K. Aziz, Ed.), p. 149, Academic Press, New York, 1975.
15. G. H. MEYER, *J. Inst. Math. Appl.* **20** (1977), 317–329.
16. G. H. MEYER, Invariant imbedding for fixed and free two point boundary value problems, in "Numerical Solution of Boundary Value Problems for Ordinary Differential Equations" (A. K., Aziz, Ed.), p. 249, Academic Press, New York, 1975.
17. G. B. WHITHAM, "Linear and Nonlinear Waves," Wiley, New York, 1974.
18. R. C. Y. CHIN AND G. W. HEDSTROM, *Math. Comp.* (to be published).